

# Supplemental Materials

*Molecular Biology of the Cell*

Brooks *et al.*

## Supplementary Figure Legends

**Figure S1:** (a) Immunofluorescence imaging of caveolin-1 (Cav-1) and cavin-1 in iso-osmotic conditions and after 5 mins of hypo-osmotic shock ( $150 \text{ mOsm L}^{-1}$ ). Scale bars  $10 \mu\text{m}$ .  
(b) Quantification of (a) shows individual junctional to cytoplasmic ratios of these proteins. Cav-1 levels at the PM are not significantly affected by hypo-osmotic shock ( $p = 0.1900$ ), whereas cavin-1 levels show a decrease of  $\sim 17\%$  ( $p = <0.0001$ ), indicative of caveolae flattening and/or dissociation.  
(c) Quantification of (a) showing the percentage change in junctional Cav-1 and cavin-1 after hypo-osmotic shock.  
(d, e) Western Blot and analysis of cavin-1 before and after hypo-osmotic shock. Protein levels are unchanged ( $p = 0.2057$ ;  $N = 3$ ), indicating that cavin-1 is redistributed from the PM, rather than undergoing degradation.  
(f) Fluorescence imaging of transient cavin-1-EGFP expression in MCF-10A epithelial monolayers under control and mechanically stretched conditions (scale bar =  $10 \mu\text{m}$ ).  
(g) Quantification of (f) reveals that 5 m of cyclic stretching at 1 Hz to a strain of 10% promotes the dissociation of  $\sim 33\%$  cavin-1 from the PM ( $p = <0.0001$ ), indicative of caveolar disassembly.  
(h) Quantification of (f) showing the percentage change in PM-associated cavin-1 following cyclic mechanical stretching of monolayers.  
(i) Amino acid sequences of undecad cavin1 (UC1) repeats from *Mus musculus* (*MmCavin1*), *Danio rerio* (*DrCavin1b*), and a modified *DrCavin1b* sequence with the deletion of four UC1 repeats (Tillu *et al.*, 2018).

All data are means  $\pm$  SD. All statistical analyses (with the exception of d, e) calculated from  $N=3$  independent experiments with 60 junctions per experiment using unpaired t-tests. Statistical analysis of d,e calculated from  $N=3$  independent western-blotting experiments. Points on graphs represent individual cell junctions. N.s, not significant; \* $p<0.05$ ; \*\* $p<0.01$ , \*\*\* $p<0.001$ ; \*\*\*\* $p<0.0001$ .

**Figure S2:** (a) Full dataset of F-actin changes in WT, Cav-1 KD, and Cav-1 KDR monolayers following hypo-osmotic shock (see figure 1a) showing data points from individual cell-cell junctions.  
(b) Full dataset of F-actin changes in WT and Cav-1 KD monolayers following mechanical stretch (see figure 1d) showing data points from individual cell-cell junctions.

All data are means  $\pm$  SD. All statistical analyses calculated from  $N=3$  independent experiments (60 junctions per experiment) using unpaired t-tests. Points on graphs represent individual cell junctions. N.s, not significant; \* $p<0.05$ ; \*\* $p<0.01$ , \*\*\* $p<0.001$ ; \*\*\*\* $p<0.0001$ .

**Figure S3:** (a) Immunofluorescent imaging of PH-Akt-GFP, a fluorescent biosensor for PtdIns (3, 4, 5) $P_3$  in WT monolayers before (left) and after (right) hypo-osmotic shock. Scale bar =  $10 \mu\text{m}$ .  
(b) Quantification of (a) showing that there is no apparent change in the level of PtdIns (3, 4, 5) $P_3$  ( $p = 0.1924$ ), the primary precursor of PtdIns(4, 5) $P_2$ , following hypo-osmotic shock.  
(c) Full dataset of junctional mCherry-PH intensity following hypo-osmotic shock (see figure 3a) showing data points from individual cell-cell junctions in WT, Cav-1 KD, and Cav-1 KDR monolayers.

All data are means  $\pm$  SD. All statistical analyses calculated from  $N=3$  independent experiments (60 junctions per experiment) using unpaired t-tests. Points on graphs represent individual cell junctions. N.s, not significant; \* $p<0.05$ ; \*\* $p<0.01$ , \*\*\* $p<0.001$ ; \*\*\*\* $p<0.0001$ .

**Figure S4:** (a) Full dataset of cavin-1 variant dissociation following hypo-osmotic shock (see figure 4b) showing data points from individual cell-cell junctions.  
(b) Full dataset of F-actin changes in monolayers expressing either the *MmCavin1*, *DrCavin1b*, or  $\Delta 4\text{UC1}$

cavin-1 variant following hypo-osmotic shock (see figure 4d) showing data points from individual cell-cell junctions.

(c) Full dataset of cavin-1 variant dissociation following exposure to calyculin A (see figure 5a) showing data points from individual cell-cell junctions.

(d) Full dataset of F-actin changes in monolayers expressing either the *MmCavin1*, *DrCavin1b*, or  $\Delta 4UC1$  cavin-1 variant following calyculin A exposure (see figure 5e) showing data points from individual cell-cell junctions.

All data are means  $\pm$  SD. All statistical analyses calculated from N=3 independent experiments (60 junctions per experiment) using unpaired t-tests. Points on graphs represent individual cell junctions. N.s, not significant; \*p<0.05; \*\*p<0.01, \*\*\*p<0.001; \*\*\*\*p<0.0001.

**Figure S5: (a)** Representative DIC imaging of WT MCF-10A epithelial monolayers treated with 50 nM calyculin A in the absence/presence of blebbistatin.



# Fig S1

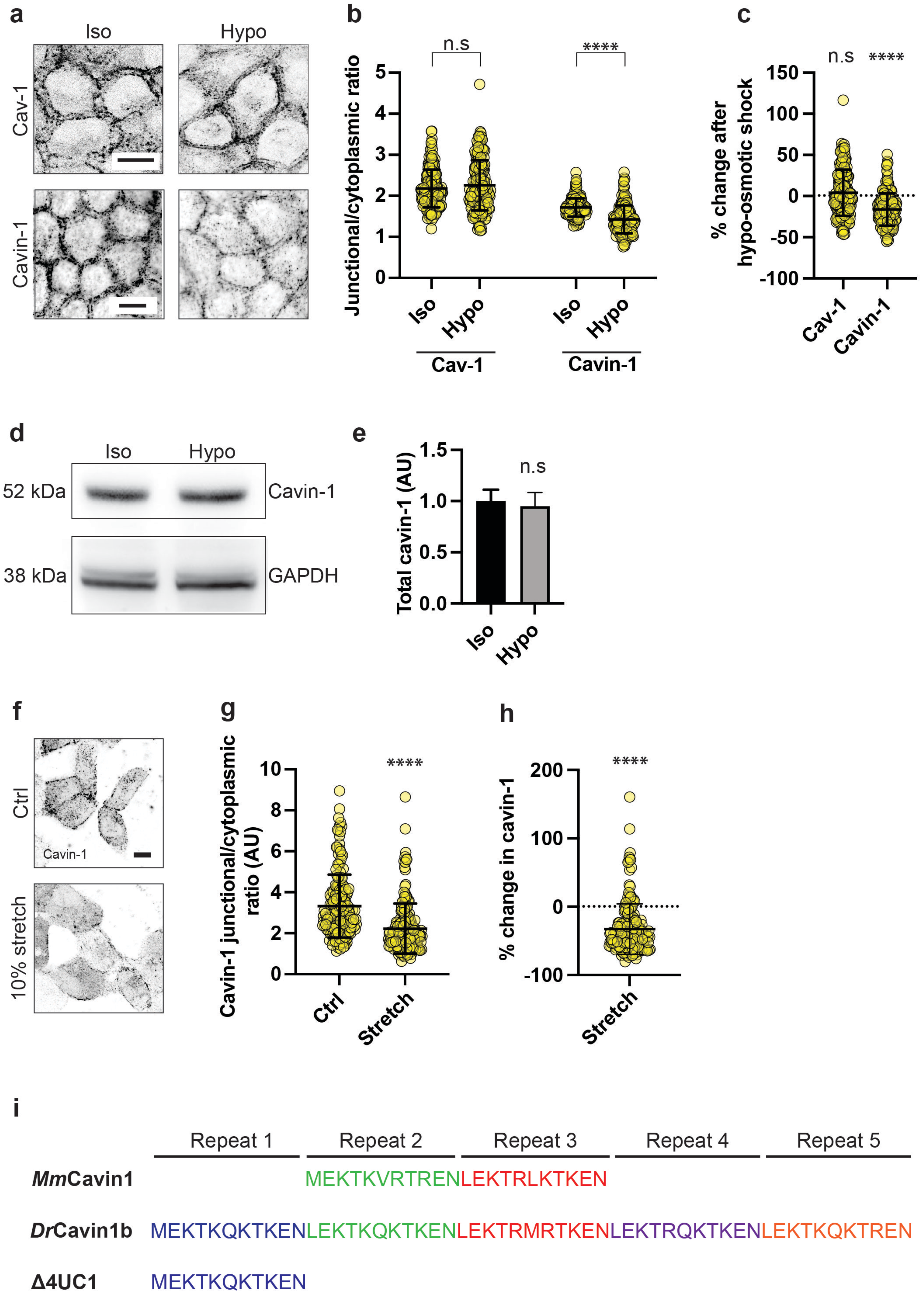
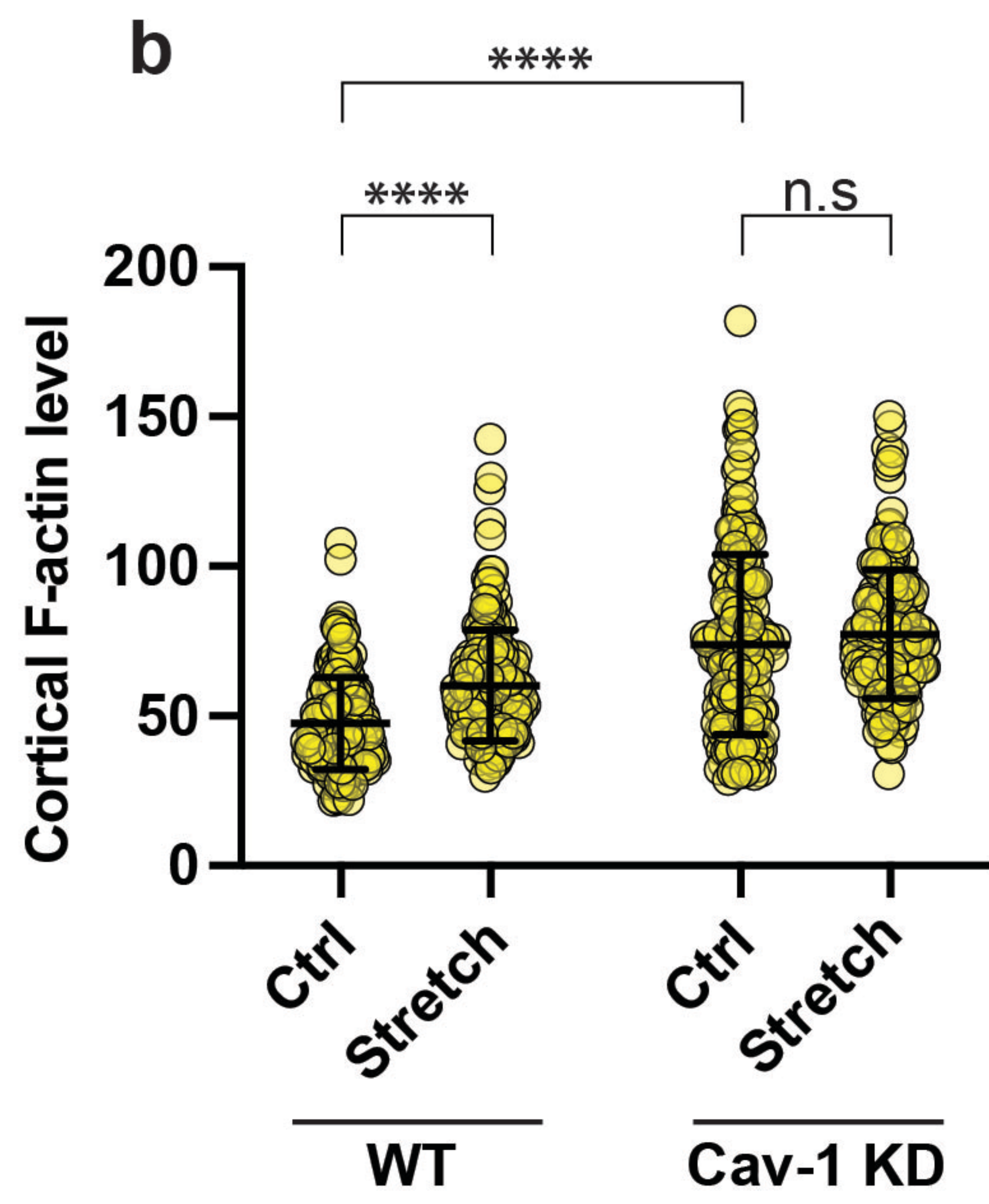
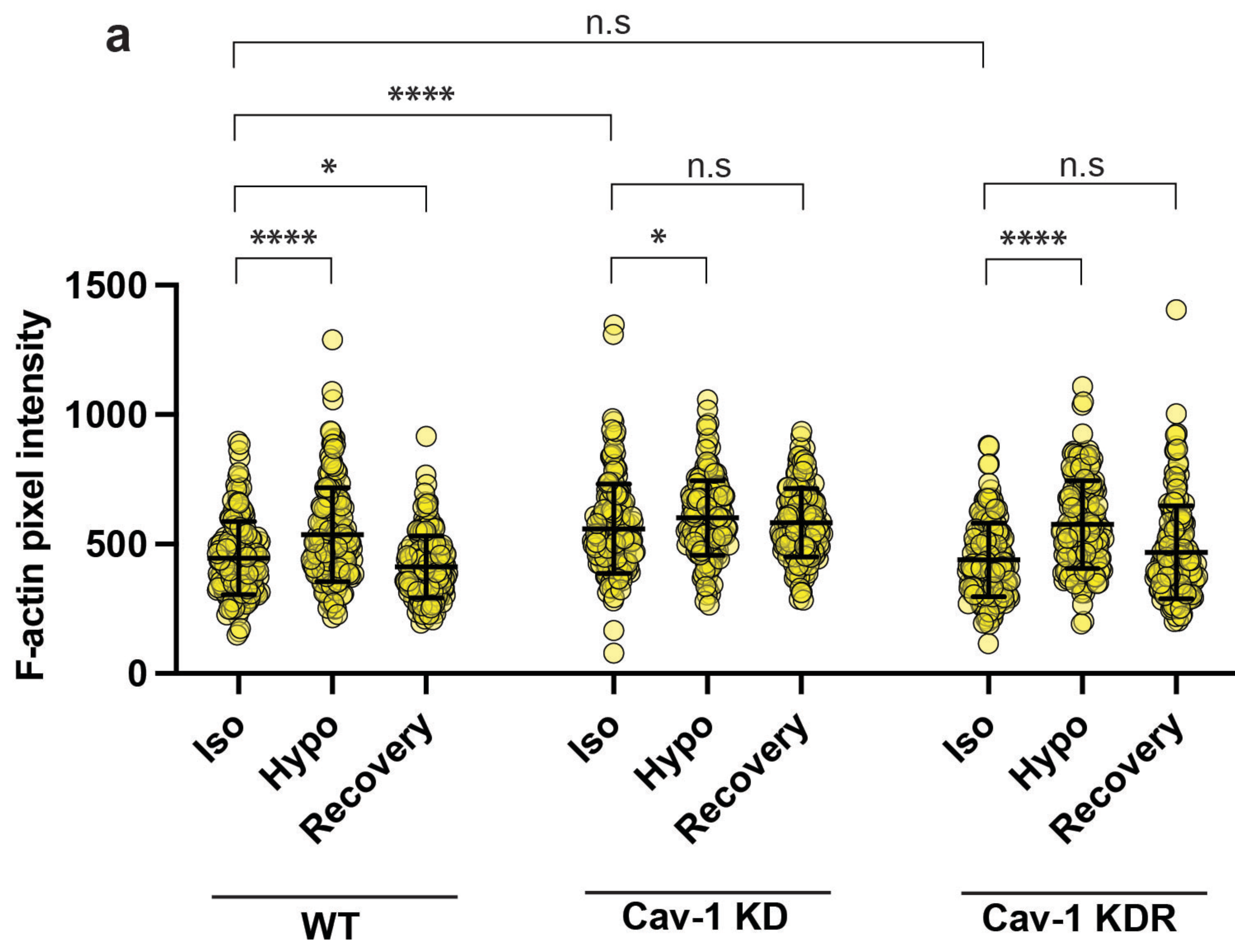


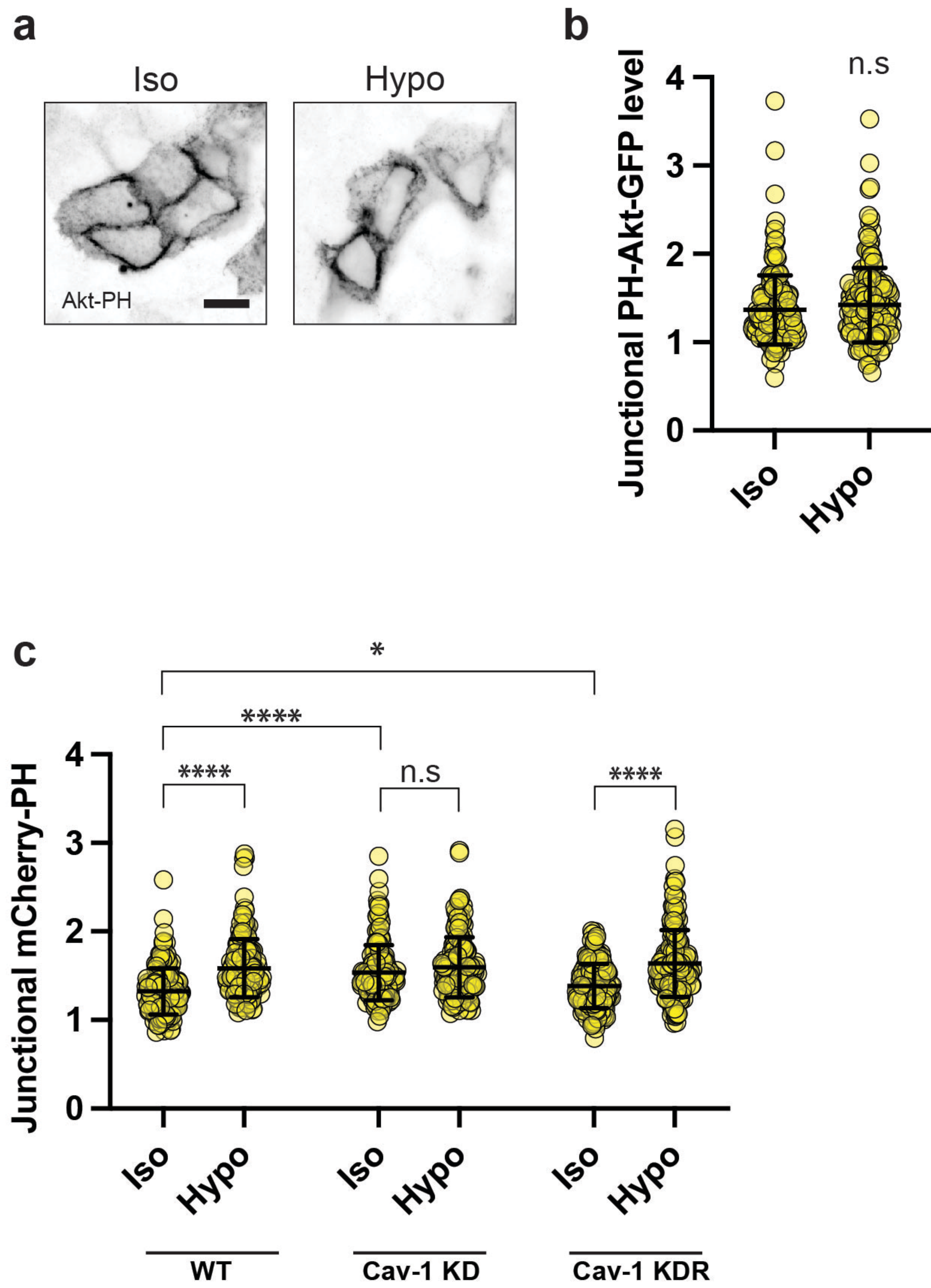


Fig S2





# Fig S3





# Fig S4

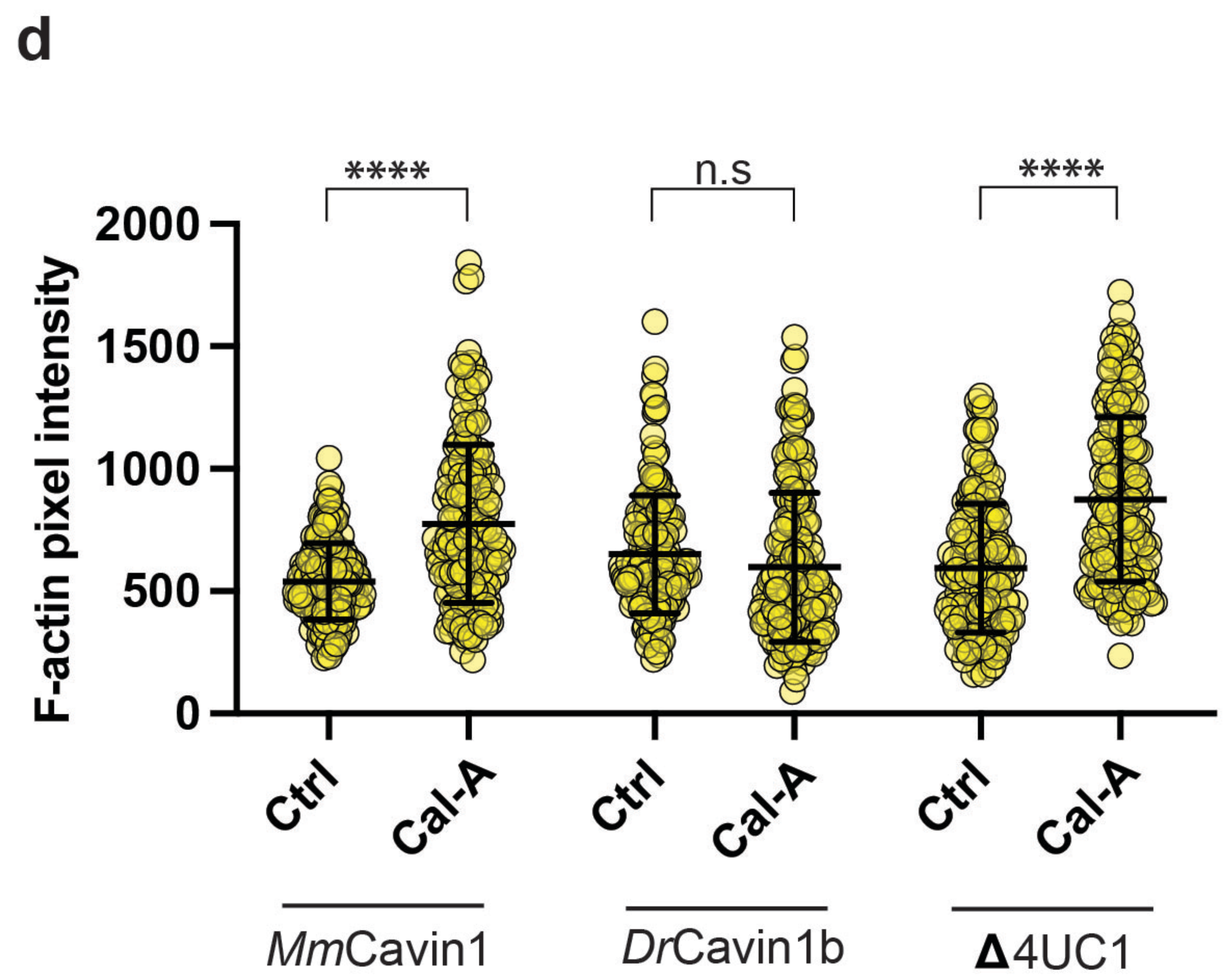
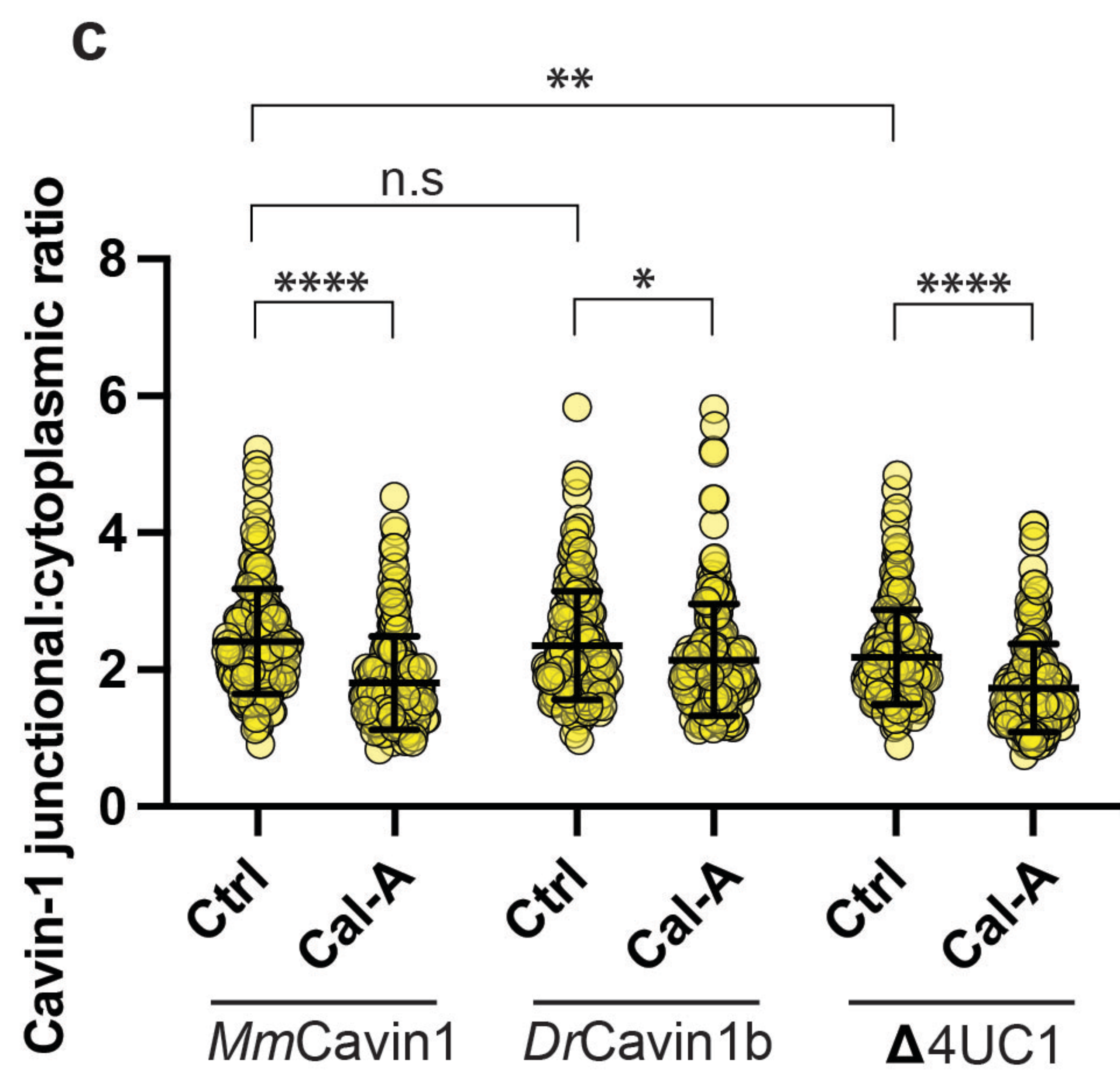
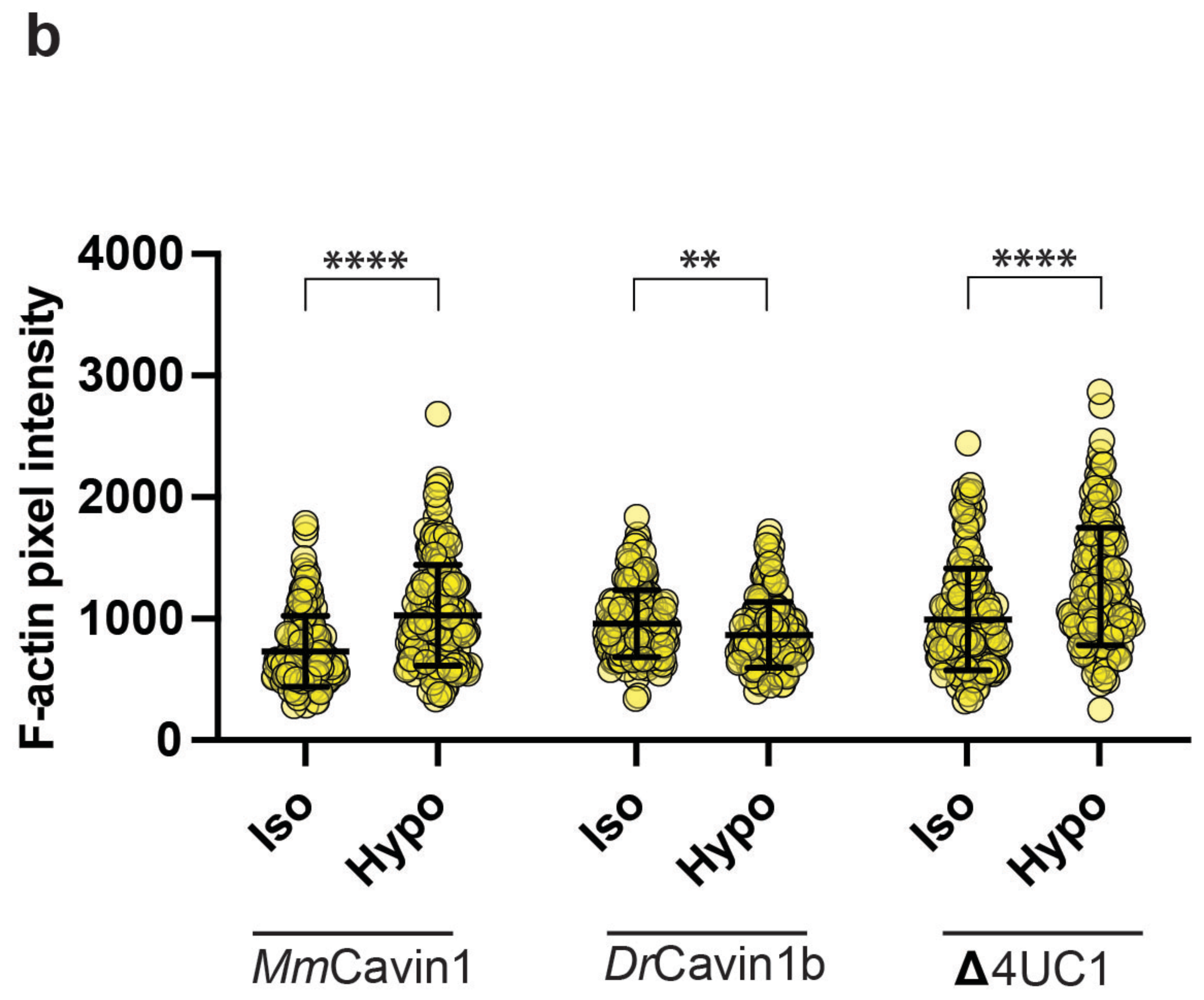
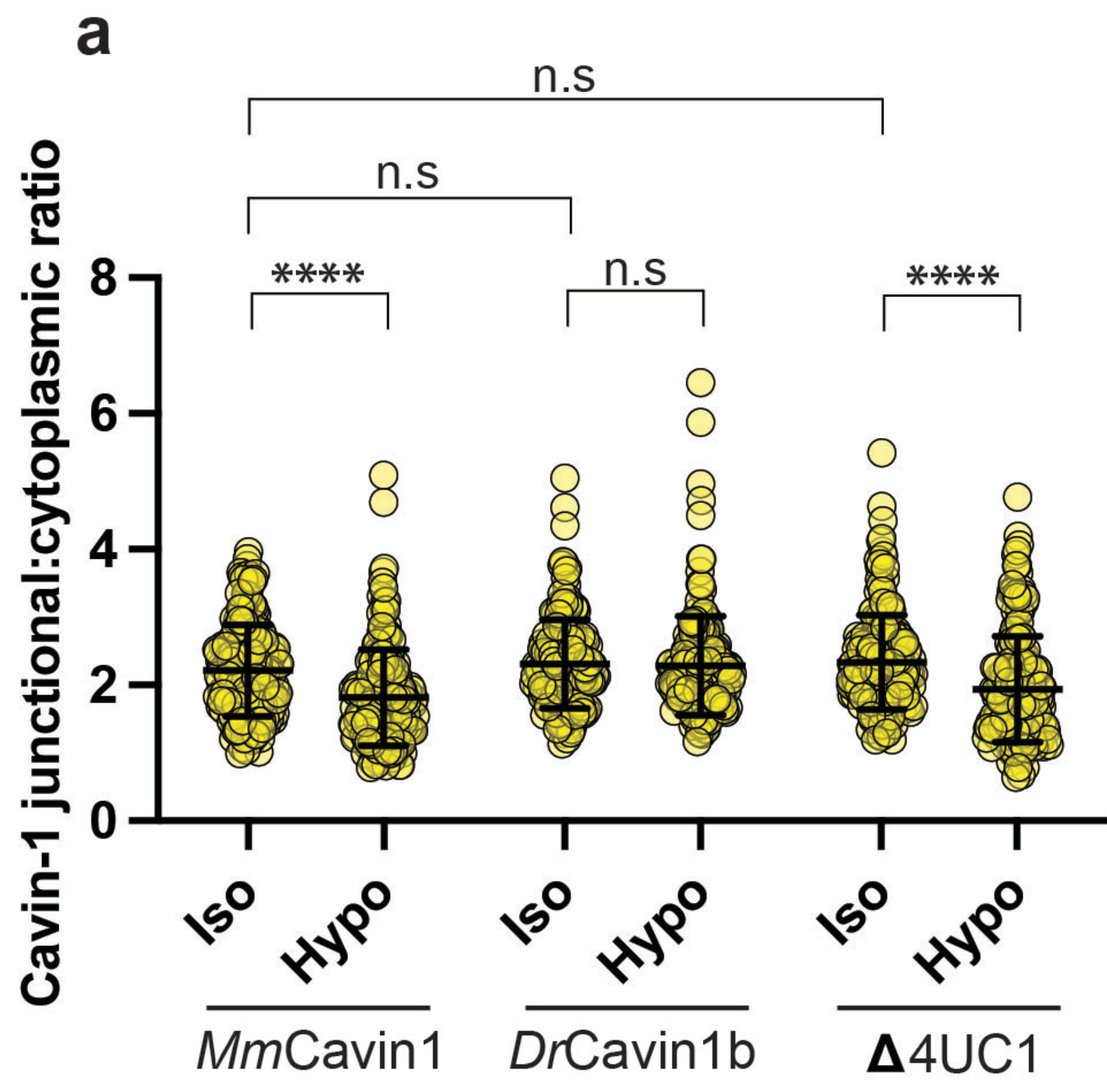




# Fig S5

